A specific subset of RabGTPases controls cell surface exposure of MT1-MMP, extracellular matrix degradation and three-dimensional invasion of macrophages

Christiane Wiesner, Karim El Azzouzi and Stefan Linder*

Institut für medizinische Mikrobiologie, Virologie und Hygiene, Universitätsklinikum Eppendorf, Martinistr. 52, 20246 Hamburg, Germany

*Author for correspondence (s.linder@uke.de)

Summary

The matrix metalloproteinase MT1-MMP has a major impact on invasive cell migration in both physiological and pathological settings such as immune cell extravasation or metastasis of cancer cells. Surface-associated MT1-MMP is able to cleave components of the extracellular matrix, which is a prerequisite for proteolytic invasive migration. However, current knowledge on the molecular mechanisms that regulate MT1-MMP trafficking to and from the cell surface is limited. We have identified three members of the RabGTPase family, Rab5a, Rab8a and Rab14, as crucial regulators of MT1-MMP trafficking and function in primary human macrophages. Both overexpressed and endogenous forms show prominent colocalisation with MT1-MMP-positive vesicles, whereas expression of mutant constructs, as well as siRNA-induced knockdown, reveal that these RabGTPases are crucial in the regulation of MT1-MMP surface exposure, contact of MT1-MMP-positive vesicles with podosomes, extracellular matrix degradation in two and three dimensions, as well as three-dimensional proteolytic invasion of macrophages. Collectively, our results identify Rab5a, Rab8a and Rab14 as major regulators of MT1-MMP trafficking and invasive migration of primary human macrophages, which could be promising potential targets for manipulation of immune cell invasion.

Key words: Cell invasion, Extracellular matrix, MT1-MMP, Podosomes, RabGTPases

Introduction

Invasive migration is a key ability of cells in both physiological and pathological scenarios, including migration of immune cells to sites of infection (Ley et al., 2007) and dissemination of cancer cells during metastasis (Friedl and Wolf, 2003; Bravo-Cordero et al., 2012). To invade, cells employ two different strategies, depending on the density of the extracellular matrix (ECM): (1) amoeboid migration, a non-proteolytic form of locomotion, with cells squeezing through the gaps between matrix fibres, and (2) mesenchymal migration, which includes degradation of matrix material (Wolf and Friedl, 2011). Both forms are not mutually exclusive, and cells can switch their behaviour according to the local ECM meshwork density (Lämmermann and Sixt, 2009; Guiet et al., 2011). The fact that *in vivo*, multiple crosslinks exist between ECM fibres, however, seems to favour the mesenchymal mode of invasion (Sabeh et al., 2009).

Particularly the matrix metalloproteinase MT1-MMP has emerged as a central regulator of proteolytic cell invasion in a variety of settings, including monocyte diapedesis (Matías-Román et al., 2005; Sithu et al., 2007), T-cell homing (Itoh and Seiki, 2004) and cancer cell metastasis (Wolf et al., 2007; Friedl and Wolf, 2008). MT1-MMP cleaves multiple matrix components, including collagen (I–III), fibronectin and fibrin (Itoh and Seiki, 2004), and also matrix receptors such as CD44, osteopontin and syndecan-1 (Kajita et al., 2001; Endo et al.,

2003). Moreover, it also proteolytically activates other MMPs such as MMP-2, MMP-8 and MMP-13 (Barbolina and Stack, 2008).

Considering the plethora of MT1-MMP functions, both the surface-associated pool of this protease and also its localised activity have to be exquisitely fine tuned. Regulatory mechanisms include: (1) adjustment of surface-associated activity by activation of pro-MT1-MMP through the convertase furin prior to its insertion into the plasma membrane (Sato et al., 1996) or inhibition by tissue inhibitors of metalloproteinases (TIMPs) or testican (Nakada et al., 2003); (2) degradation of MT1-MMP, which can be induced by autolysis (Lehti et al., 1998) or MMP-2 (Stanton et al.,1998); and (3) vesicle-mediated regulation of the surface-associated MT1-MMP pool, which is influenced by furin-induced uptake (Remacle et al., 2006), by PKC-dependent phosphorylation of Thr567, leading to enhanced internalisation (Williams and Coppolino, 2011), or by active Rab8, which leads to enhanced exocytosis (Bravo-Cordero et al., 2007).

In consequence, vesicle-mediated transport of MT1-MMP plays a key role in the regulation of surface-localised MT1-MMP activity, both through exocytic delivery of the proteinase and also by endocytic internalisation (Frittoli et al., 2011). Regulators of vesicle formation, transport and fusion are thus expected to have a major impact on MT1-MMP trafficking and, ultimately, on

proteolytic cell invasion. Several components of the respective molecular machineries have already been described: in primary macrophages, MT1-MMP-positive vesicles travel bidirectionally along microtubules, in a process driven by kinesin-1 and -2 motors, as well as by cytoplasmic dynein, which regulates cell surface exposure of MT1-MMP (Wiesner et al., 2010). In MDA-MB-231 breast cancer cells, trafficking of MT1-MMP to matrix-degrading invadopodia is regulated by the SNARE protein VAMP-7. Consequently, siRNA-mediated knockdown of VAMP-7 resulted in decreased invasive capacity of these cells (Steffen et al., 2008; Poincloux et al., 2009), a phenomenon that has also been observed in HeLa cells (Williams and Coppolino, 2011).

RabGTPases are central regulators of both endocytosis and exocytosis of vesicles (Schwartz et al., 2007; Stenmark, 2009; Hutagalung and Novick 2011). Depending on their nucleotide-bound state, RabGTPases act as molecular switches (Stenmark et al., 1994) that mediate specific tethering of vesicles to target organelles, thus ensuring correct compartmentalisation of cargo proteins (Zerial and McBride, 2001). Currently, more than 70 mammalian Rab proteins are known (Hutagalung and Novick, 2011). However, despite their pivotal importance for multiple aspects of intracellular transport (Stenmark, 2009; Hutagalung and Novick 2011), knowledge of the impact of RabGTPases on the trafficking of MT1-MMP is limited. The only well-documented cases concern, (1) MDA-MB-231 breast carcinoma cells, where MT1-MMP localised to Rab8-positive vesicles, and siRNA-mediated knockdown of Rab8 inhibited collagen degradation and invasion (Bravo-Cordero et al., 2007), and (2) HT1080 fibrosarcoma cells, where MT1-MMP localised to Rab5- and Rab7-positive compartments, and overexpression of dominant negative Rab7 led to a reduction of surface-associated MT1-MMP and also of cell invasion (Williams and Coppolino, 2011).

Here, we present novel data on the impact of several specific RabGTPases on MT1-MMP trafficking and function in primary human macrophages. We show that overexpression of mutants as well as siRNA-induced knockdown of Rab5a, Rab8a and Rab14 critically regulate cell surface exposure of MT1-MMP, contact of MT1-MMP-positive vesicles with podosomes, as well as podosome-localised ECM degradation in two and three dimensions, and also three-dimensional (3D) proteolytic invasion. Our results thus identify three RabGTPases with a major impact on MT1-MMP trafficking and proteolytic invasion of macrophages, which could be promising targets for therapeutic modulation of macrophage invasion.

Results

MT1-MMP vesicles are positive for Rab5a, Rab8a, Rab14, Rab21 and Rab22a

To identify RabGTPases involved in MT1-MMP trafficking in primary human macrophages, we first performed co-expression experiments with a variety of GFP-fused Rab constructs together with MT1-MMP-mCherry. In fixed cells, pronounced localisation at MT1-MMP–mCherry-positive vesicles was found for GFP–Rab5a, GFP–Rab8a, GFP–Rab14, GFP–Rab21 and GFP–Rab22a (Fig. 1). In case of GFP–Rab5a, GFP–Rab14, GFP–Rab21 and GFP–Rab22a overexpression, we also observed the formation of giant vesicles (Fig. 1A–C,G–O), as previously reported for a variety of cell types (Stenmark et al., 1994; Olkkonen et al., 1993; Junutula et al., 2004; Pellinen et al., 2006). This phenomenon also allowed higher spatial resolution of vesicle subdomains, and
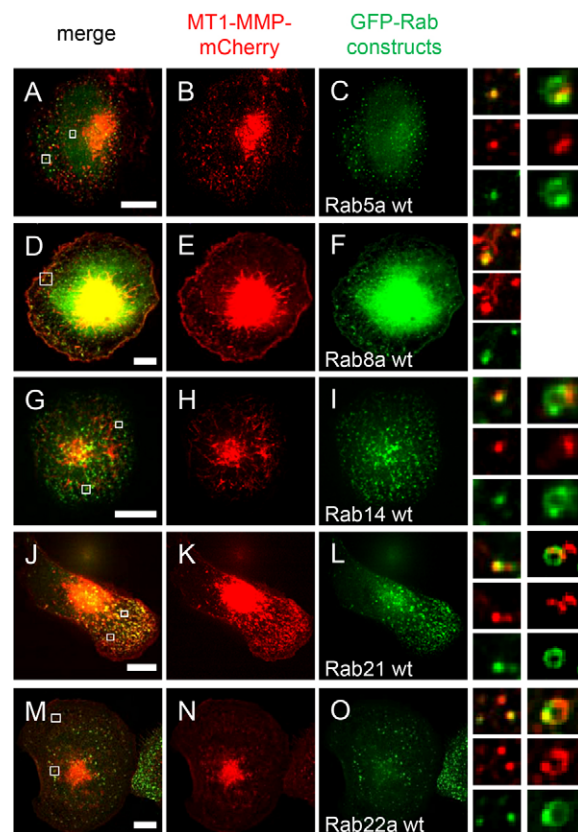
Fig. 1. MT1-MMP–mCherry vesicles partially colocalise with Rab5a, Rab8a, Rab14, Rab21 and Rab22a wild-type constructs. Confocal micrographs of macrophages expressing MT1-MMP–mCherry and GFP–Rab5a (**A–C**), GFP–Rab8a (**D–F**), GFP–Rab14 (**G–I**), GFP–Rab21 (**J–L**), or GFP–Rab22a (**M–O**). Merged images are shown in the left column, with single channel images of MT1-MMP–mCherry shown in middle column (red) and of GFP-fused Rab GTPases in right column (green). The regions in the white boxes in the merged images are shown enlarged on the right. Note localisation of MT1-MMP–mCherry together with Rab constructs on vesicles (left column of enlarged images) and giant vesicles (right column of enlarged images; fused vesicles are due to the overexpression of GFP–RabGTPase). The enlarged images in the left column show 1–4 individual vesicles; those in the right column show a single giant vesicle. Scale bars: 10 μm.

revealed that MT1-MMP and RabGTPases show distinct, although partially overlapping, localisations at these vesicles (Fig. 1A–C,G–O). (Note that localisation of RabGTPases and MT1-MMP at the same vesicles does not necessarily imply colocalisation of the respective signals, as they mostly segregate to different domains on these vesicles.)

Live cell imaging experiments in cells transfected with respective constructs confirmed that the identified RabGTPases localise to dynamic vesicles that are also positive for MT1-MMP–mCherry (supplementary material Fig. S1; Movies 1, 2). Moreover, colocalisation studies of endogenous proteins in cells stained with specific primary antibodies against MT1-MMP and RabGTPase isoforms (supplementary material Fig. S2) confirmed the results of the overexpression screen and demonstrated that Rab5, Rab8a, Rab14, Rab21 and Rab22a show substantial colocalisation with MT1-MMP vesicles. The identified RabGTPases are thus potential candidates for the regulation of MT1-MMP trafficking in primary human macrophages. (Note:

several other tested RabGTPases, including Rab4, Rab6a, Rab9 and Rab11, showed no colocalisation at MT1-MMP vesicles (see supplementary material Fig. S3) and were thus mostly not investigated further. (See supplementary material Fig. S9 for proof-of-principle experiments showing that the non-colocalising isoform Rab6a does not influence surface exposure of endogenous MT1-MMP, 3D collagen degradation or 3D matrix invasion.)

Cell surface exposure of MT1-MMP is regulated by Rab5a, Rab8a, Rab14 and Rab22a

In a next step, we overexpressed dominant active (DA) and negative (DN) mutants of the identified RabGTPases and analysed their potential effects on the cell surface exposure of MT1-MMP–mCherry. Non-permeabilised cells overexpressing the respective constructs were labelled with an anti-mCherry antibody, detecting the intramolecular mCherry tag of MT1-MMP–mCherry, which had been subcloned N-terminally of the MT1-MMP transmembrane domain, and is thus extracellularly accessible on the surface-exposed protein (Wiesner et al., 2010; Sakurai-Yageta et al., 2008). Fluorescence intensities were measured and the ratio of cell surface associated versus total cellular MT1-MMP–mCherry was used as a parameter for the cell surface exposure of MT1-MMP. Cells expressing respective GFP-fused wild-type constructs were used as controls. In all cases, RabGTPase expression levels, as judged by GFP-based fluorescence levels (supplementary material Fig. S4), were found to be comparable.

Pronounced deviations of the surface/total MT1-MMP–mCherry ratio were found upon expression of DN mutants of Rab5a, Rab8a, Rab14 and Rab22a. Dominant negative Rab21 and all respective DA mutants showed no or only minor effects (for specific values, see supplementary material Table S1). Interestingly, expression of GFP–Rab5aDN led to an increase of surface-associated MT1-MMP–mCherry (199.9±83.2%; Fig. 2D), whereas a decrease was measured for GFP–Rab8aDN (40.7±18.6%; Fig. 2H), GFP–Rab14DN (53.4±16.8%; Fig. 2L) and GFP–Rab22aDN (27.5±12.0%; Fig. 2T).

We next measured the impact of these RabGTPase mutants on the cell surface exposure of endogenous MT1-MMP. Cells expressing respective RabGTPase constructs were fixed, but not permeabilised, and stained for surface-associated MT1-MMP using a specific primary antibody (note that this antibody is directed against an epitope in the catalytic domain and thus recognises only unshed, but not cleaved, MT1-MMP on the cell surface). Comparable to the results gained for MT1-MMP–mCherry, we found a pronounced increase of surface-associated endogenous MT1-MMP upon expression of GFP–Rab5aDN (173.5±80.3%; supplementary material Fig. S5D), and pronounced decreases upon expression of GFP–Rab8aDN (76.8±25.0%; supplementary material Fig. S5H), GFP–Rab14DN (68.2±22.7%; supplementary material Fig. S5L) and GFP–Rab22aDN (43.9±24.9%; supplementary material Fig. S5T). Expression levels of the respective RabGTPase constructs were comparable (supplementary material Fig. S5U–Y).

To address the role of the identified Rab proteins in MT1-MMP surface exposure directly, we established respective siRNA-mediated knockdowns. For each identified RabGTPase,
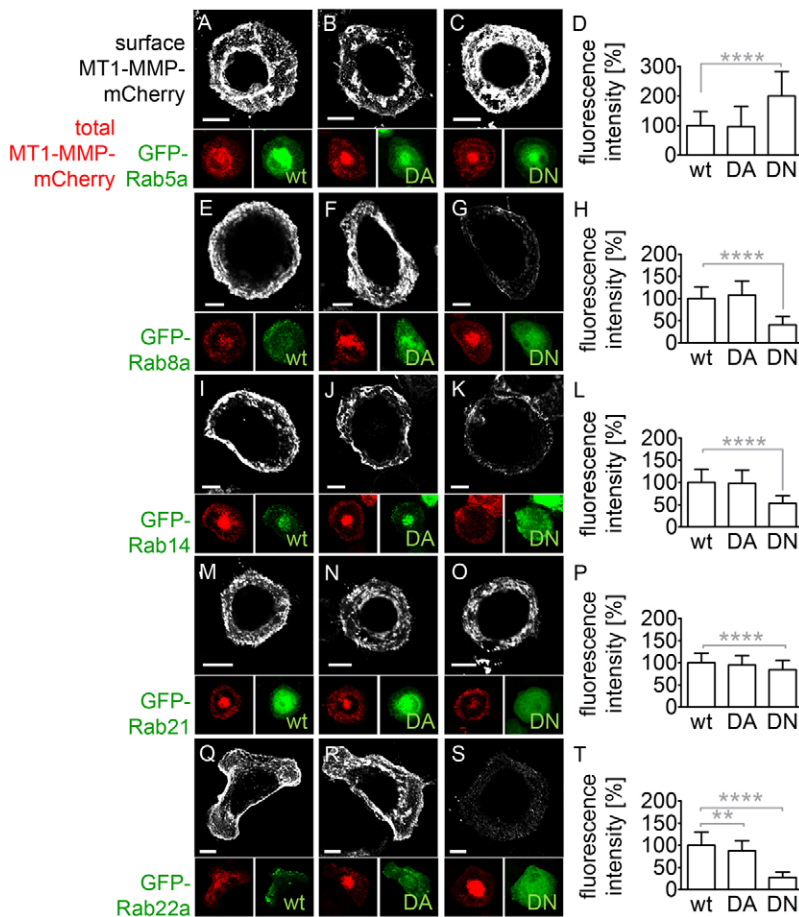
Fig. 2. Cell surface exposure of MT1-MMP–mCherry is regulated by Rab5a, Rab8a, Rab14 and Rab22a, but not Rab21. (A–C, E–G, I–K, M–O, Q–S) Confocal micrographs of macrophages coexpressing MT1-MMP–mCherry (red) and GFP-fused RabGTPase constructs (green): wild-type (A,E,I,M,Q; green), dominant active (DA) constructs deficient in GTP hydrolysis (B,F,J,N,R; green), or dominant negative constructs (DN) deficient in GTP binding (C,G,K,O,S; green). Cells were fixed, but not permeabilised, and stained with primary anti-mCherry antibody and secondary Alexa-Fluor-647-conjugated antibody to label surface-associated MT1-MMP–mCherry (white). Note pronounced reduction of MT1-MMP at cell surface upon overexpression of Rab8a, Rab14, Rab22a DN mutants, but less in the Rab21 DN mutant. Note also increased cell surface exposure of MT1-MMP in case of Rab5a DN and Rab7a DN overexpression. Scale bars: 10 μm for all images of the same row. (D,H,L,P,T) Evaluation of fluorescence intensities of surface-localised MT1-MMP–mCherry, based on Alexa Fluor 647 fluorescence, relative to the intensity of total MT1-MMP–mCherry fluorescence. Values for wild-type constructs were to 100%. 3×30 (n=90; from 3 different donors) cells were evaluated. Graphs show means + s.d. Asterisks indicate values significantly different from wild-type constructs: **P<0.002, ****P<0.0001. For specific values, see supplementary material Table S1.
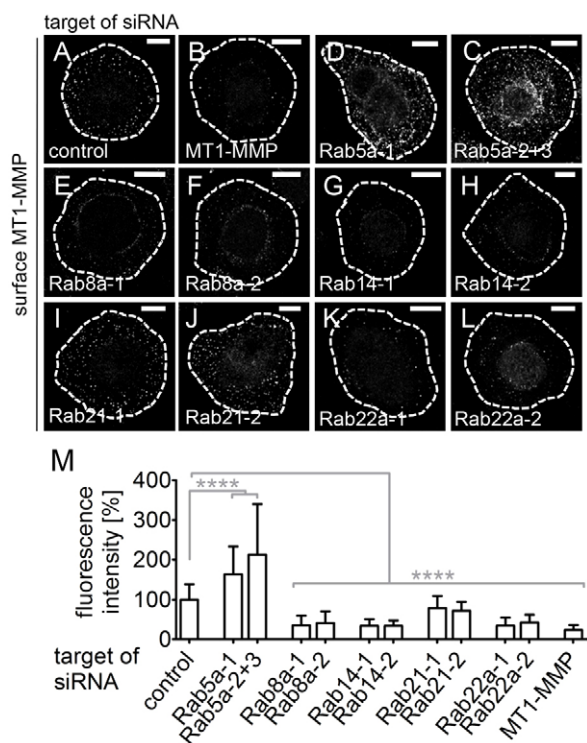
two independent siRNAs were generated (three in case of Rab5a), and the respective decrease in protein levels was shown on Western blots of macrophage lysates. Knockdown efficiencies ranged from 42% to 96%, with at least one of the two independent siRNAs leading to a knockdown of ca. 80% (supplementary material Fig. S6). Importantly, knockdown of these RabGTPase isoforms did not change the overall levels of cellular MT1-MMP (supplementary material Fig. S6). Cells treated with the respective siRNAs were fixed, but not permeabilised, and stained for surface-exposed endogenous MT1-MMP, with cells treated with luciferase- or MT1-MMP-specific siRNA (Wiesner et al., 2010) used as negative or positive controls (Fig. 3; for specific values, see supplementary material Table S1), respectively. Comparable to the expression of DN mutants, knockdown of Rab5a led to a significant increase of cell surface-exposed MT1-MMP ($163.1\pm70.1\%$ and $212.7\pm127.2\%$), whereas pronounced decreases were observed upon knockdown of Rab8a ($35.3\pm24.3\%$ and $41.3\pm29.5\%$), Rab14 ($33.9\pm17.0\%$ and $34.1\pm13.3\%$) and Rab22a ($34.6\pm20.3\%$ and $42.7\pm19.4\%$; Fig. 3M). A less pronounced but still significant effect was observed upon knockdown of Rab21 ($78.6\pm31.0\%$ and

Fig. 3. **Knockdown of Rab5a, Rab8a, Rab14 and Rab22a, but not of Rab21 has a major impact on the cell surface exposure of endogenous MT1-MMP.** (A–L) Confocal micrographs of macrophages treated with siRNA specific for luciferase, as control (A), MT1-MMP (B), or RabGTPase isoforms, as indicated. Cells were fixed, but not permeabilised, and stained with primary anti-MT1-MMP and secondary Alexa-Fluor-568-conjugated antibody to label endogenous MT1-MMP on the cell surface. Scale bars: 10 μm. (M) Fluorescence intensities of surface-localised endogenous MT1-MMP, based on Alexa Fluor 568 fluorescence. Fluorescence intensities for control siRNA were each set to 100%. For all values, 30 cells from three different donors each were evaluated. Graph shows means + s.d. Asterisks indicate values significantly different from control values: ****$P<0.0001$. For specific values, see supplementary material Table S1.

$72.1\pm22.8\%$). We conclude from these experiments that especially Rab5a, Rab8a, Rab14 and Rab22a are important regulators of cell surface exposure for both endogenous and overexpressed MT1-MMP in primary macrophages.
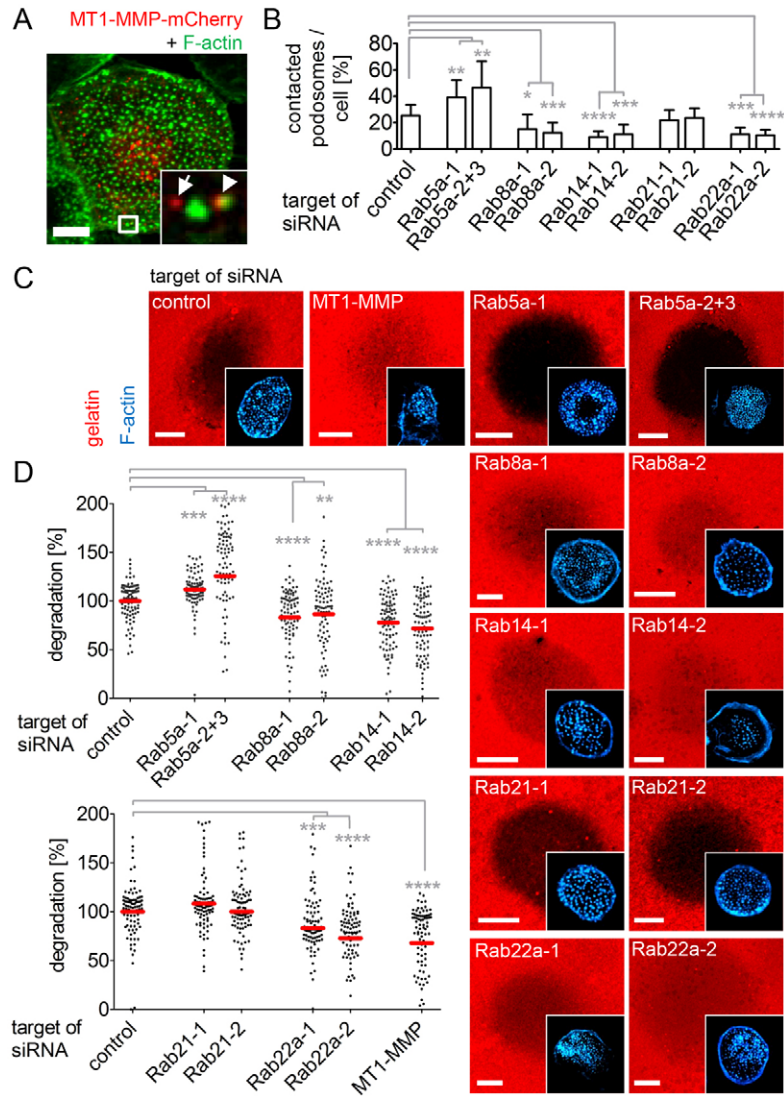
Podosome contact of MT1-MMP vesicles and podosomal matrix degradation are regulated by Rab5a, Rab8a, Rab14 and Rab22a

A major surface-associated function of MT1-MMP is degradation of the extracellular matrix (van Hinsbergh et al., 2006; Wolf and Friedl, 2009). In monocytic cells, this is achieved by MT1-MMP-dependent, localised proteolysis of ECM material at podosomes, the major degradative organelles of macrophages and other invasive cell types (Linder et al., 2011; Murphy and Courtneidge, 2011). Delivery of MT1-MMP to podosomes is mediated by trafficking of MT1-MMP-positive vesicles along microtubules (Wiesner et al., 2010). To test the potential influence of the identified RabGTPases on this process, we evaluated contact events of MT1-MMP-positive vesicles with podosomes upon knockdown of Rab5a, Rab8a, Rab14, Rab21 and Rab22a. Three days after transfection with respective siRNAs, cells were transfected with MT1-MMP-mCherry, cultured for an additional day, fixed and stained with Alexa-Fluor-488–phalloidin to detect F-actin-rich podosome cores. The number of podosomes that were in direct contact with MT1-MMP–mCherry-positive vesicles (Fig. 4A) was counted, and set in relation to the total number of podosomes within a cell (usually >100; ratio of contacted podosomes: $25.3\pm8.1\%$). Strikingly, knockdown of Rab5a led to a higher ratio of podosomes contacted by MT1-MMP–mCherry vesicles ($39.1\pm13.0\%$ and $46.4\pm20.0\%$), whereas the ratios of contacted podosomes were significantly decreased upon knockdown of Rab8a ($15.2\pm11.0\%$ and $12.3\pm7.6\%$), Rab14 ($9.1\pm4.4\%$ and $11.1\pm7.3\%$) and Rab22a ($11.1\pm5.3\%$ and $10.4\pm4.1\%$), but not of Rab21 ($21.8\pm7.8\%$ and $23.6\pm7.3\%$; Fig. 4B). Importantly, overall cellular expression of MT1-MMP–mCherry as well as overall podosome number in cells were unchanged upon knockdown of the mentioned RabGTPases (supplementary material Fig. S7 and not shown).

To explore potential functional consequences, we next assessed podosome-associated matrix degradation under knockdown of specific RabGTPases. Cells were treated with respective siRNAs for 3 days re-seeded on Rhodamine-labelled gelatine matrix for 6 h, fixed and stained for F-actin to label podosome cores, and podosome-dependent ECM degradation was assessed by associated loss of the Rhodamine matrix label (Fig. 4C). Cells treated with luciferase- or MT1-MMP specific siRNAs were used as negative or positive controls, respectively, with values for luciferase-treated cells set to 100%. Knockdown of endogenous MT1-MMP led to significantly decreased levels of gelatine matrix degradation ($67.9\pm35.5\%$), comparable to earlier results in macrophages (Wiesner et al., 2010). Consistent with the results gained for podosome contact of MT1-MMP vesicles, knockdown of Rab5a led to significantly enhanced levels of matrix degradation ($111.9\pm18.7\%$ and $125.6\pm59.5\%$), whereas pronounced decreases in matrix degradation were measured upon knockdown of Rab8a ($82.9\pm30.6\%$ and $86.4\pm38.0\%$), Rab14 ($77.7\pm28.2\%$ and $71.8\pm31.8\%$) and Rab22a ($83.1\pm37.2\%$ and $72.8\pm37.5\%$), but not of Rab21 ($108.3\pm37.4\%$ and $100.0\pm36.5\%$; Fig. 4D). Collectively, these results indicate that Rab5a acts as negative regulator of MT1-MMP vesicle contact

Fig. 4. Knockdown of Rab5a, Rab8a, Rab14 and Rab22a, but not of Rab21, affects contact of MT1-MMP–mCherry vesicles with podosomes and matrix degradation. (**A**) Confocal micrograph of a primary macrophage expressing MT1-MMP–mCherry and stained for F-actin using Alexa-Fluor-488–phalloidin to highlight podosome cores. The region in the white box is enlarged in the inset. Scale bar: 10 μm. White arrow or arrowhead indicate MT1-MMP–mCherry vesicles not in contact or in contact with a podosome, respectively. (**B**) Quantification of podosomes contacted by MT1-MMP–mCherry vesicles per cell. Total number of podosomes was set to 100%. For all values, five cells from three different donors each with 50–500 podosomes were evaluated. Graph shows means + s.d. Asterisks indicate values significantly different from control values: *$P<0.02$, **$P=0.005$, ***$P<0.0005$, ****$P<0.0001$. For specific values, see supplementary material Table S1. (**C**) Confocal micrographs of macrophages transfected with siRNA specific for RabGTPase isoforms, luciferase as negative control, or MT1-MMP as positive control, and seeded on Rhodamine-labelled gelatine matrix. Matrix degradation is visible as dark areas by concomitant loss of the fluorescent label. Insets show respective F-actin staining by Alexa-Fluor-647-labelled phalloidin. Scale bar: 10 μm. (**D**) Statistical evaluation of matrix degradation in cells treated with various siRNAs. The degree of matrix degradation was analysed by fluorescence measurements of 30 cells from three different donors each for each value. Red bars indicate mean values, black dots show single values; Mean value of matrix degradation in control was set as 100%. Asterisks indicate values significantly different from control value: **$P=0.003$, ***$P<0.0009$, ****$P<0.0001$. For specific values, see supplementary material Table S1.

with podosomes, and also of podosomal matrix degradation, while Rab8a, Rab14 and Rab22a are positive regulators of these processes.

Matrix degradation in 3D is localised at podosome equivalents and is regulated by Rab5a, Rab8a, Rab14 and Rab22a

Within tissues, cells are surrounded by a 3D environment. This most likely affects both regulatory pathways involved in matrix degradation as well as the matrix-degrading organelles themselves, compared to 2D situations. To date, the formation of matrix-degrading podosome equivalents in 3D is very likely (Linder et al., 2011; Van Goethem et al., 2010), although unproven. To explore the possible formation of podosome-like structures in macrophages also in a 3D context, we embedded cells expressing MT1-MMP-mCherry and LifeAct-GFP (for visualisation of F-actin) in 3D collagen I and assessed the localisation of these constructs (Fig. 5A). Consistent with previous reports (Van Goethem et al., 2010; Vérollet et al., 2011), we found formation of elongated protrusions, which showed F-actin enrichment at their tips. Strikingly, the tips were also enriched in MT1-MMP–mCherry, pointing to a potential degradative capacity

of these structures (Fig. 5A). We assessed the possibility by co-staining of endogenous, surface-exposed MT1-MMP and of cleaved collagen I, using an antibody that detects a neoepitope in degraded collagen I (Wolf and Friedl, 2005). These stainings demonstrated that many of the MT1-MMP enriched protrusions are also sites of cleavage of the extracellular matrix (Fig. 5B).

We proceeded to quantify matrix degradation by macrophages in a 3D context, using a collagen dequenching assay, to evaluate the potential influence of the identified RabGTPases on this process. Macrophages were treated with RabGTPase isoform-specific siRNAs, or luciferase- or MT-MMP-specific siRNA as controls, cultured for 3 days, and embedded in quenched collagen I matrix. In this assay, collagen fibres are densely labelled by fluorophores, which effectively quenches their fluorescence. Only after proteolytic cleavage, distance between fluorophores is increased, and the matrix, and also cells that take up matrix material, become fluorescent (Fig. 5C). This increase in fluorescence can be used as a quantitative parameter for ECM degradation (Wolf et al., 2003). Matrix with embedded control cells treated with luciferase siRNA showed progressive increases in fluorescence (1129.9 ± 111.8 a.u. at 36 h), indicative of ongoing ECM degradation. This was significantly decreased to
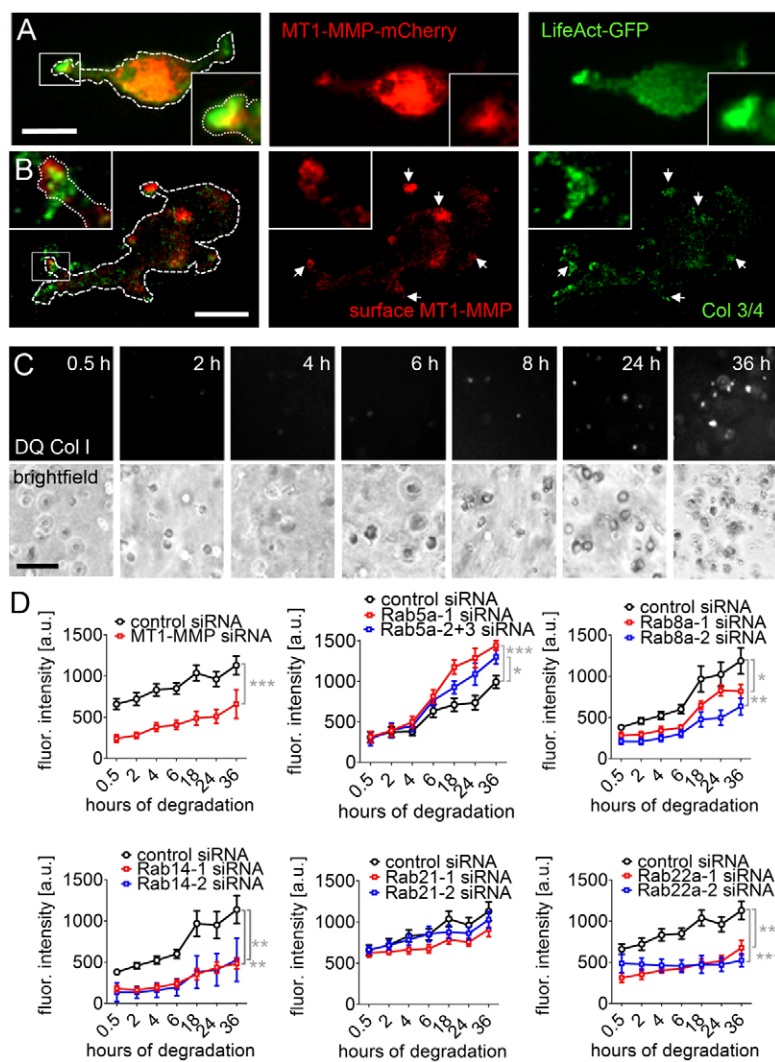
Fig. 5. 3D collagen I degradation is regulated by Rab5a, Rab8a, Rab14 and Rab22a, but not Rab21. (**A**) Confocal micrograph of a macrophage expressing MT1-MMP–mCherry (red) and LifeAct–GFP (green; to visualize F-actin) embedded in collagen I. Dashed white line indicates cell outline. White box indicates the region enlarged in the insert showing a cellular protrusion enriched in MT1-MMP–mCherry and F-actin. Scale bar: 10 µm. (**B**) Confocal 3D reconstruction of a macrophage embedded in collagen I, fixed 18 h post seeding and stained with primary antibodies against MT1-MMP (targeting surface MT1-MMP; red) and collagen 3/4 (green; to visualize degradation of ECM) and secondary antibodies coupled with Alexa Fluor 568 and Alexa Fluor 488, respectively. Dashed white lines indicate cell outline. White box indicates the region enlarged in the insert showing a cellular protrusion enriched in MT1-MMP and degradation of collagen I; further accumulations of MT1-MMP and collagen I degradation are marked by arrows. Scale bar: 10 µm. (**C**) Fluorescence (upper row) and brightfield (lower row) micrographs of macrophages embedded in quenched DQ collagen I matrix. Time after start of experiment is indicated. Scale bar: 50 µm. (**D**) Quantification of dequenched collagen I fluorescence, indicative of progressive matrix proteolysis, in cells treated with the indicated siRNAs. In all experiments, two siRNAs against each protein were used (blue and red lines and symbols), and control cells treated with luciferase siRNA were used in parallel (black lines and symbols). Cells treated with MT1-MMP-specific siRNA were used as positive control. Fluorescence intensities are given in arbitrary units (a.u.). Graphs show means + s.e.m. Time after start of experiment is indicated. Asterisks indicate values significantly different from control value at 36 h: *P<0.018, **P<0.008, ***P<0.006. For all values, 3×48 measurements were evaluated. For specific values, see supplementary material Table S1.

ca. 50% in cells treated with MT1-MMP-specific siRNA (659.6±173.8 a.u. at 36 h; Fig. 5D). Importantly, matrix degradation was also decreased to comparable levels in case of knockdown of Rab8a (818.9±84.5 a.u. and 635.4±102.5 a.u. at 36 h), Rab14 (482.67±63.77 a.u. and 528.17±75.58 a.u. at 36 h) and Rab22a (676.1±88.7 a.u. and 524.7±76.9 a.u. at 36 h), but not of Rab21 (910.7±89.8 a.u. and 1027.6±100.3 a.u. at 36 h). In contrast, knockdown of Rab5a resulted in an increase of matrix degradation (879.3±66.5 a.u. and 762.7±78.5 a.u. at 36 h). We conclude that macrophages form F-actin rich podosome equivalents in 3D, which are enriched in MT1-MMP and are able to locally degrade ECM material. Comparable to the situation in 2D, matrix degradation in 3D is negatively regulated by Rab5a, and positively regulated by Rab8a, Rab14 and Rab22a.

3D invasion of macrophages is regulated by Rab5a, Rab8a and Rab14

Proteolytic matrix degradation is a prerequisite, but not the only determinant, for successful mesenchymal invasion (Wolf and Friedl, 2011; Petrie et al., 2012). We thus assessed the potential influence of the identified RabGTPases on this complex cellular behaviour in 3D. For this, we established a 3D invasion assay, in which cells are embedded in a plug of dense collagen I, which is

surrounded by a shell of less dense collagen I. M-CSF in the outer shell acts as a chemoattractant, promoting invasion (Fig. 6A; supplementary material Fig. S10). Time lapse videomicroscopy showed that primary macrophages successfully invade the outer shell along the whole length of the plug, leading to invasive migration in several optical planes (Fig. 6B; supplementary material Movie 3). Moreover, invading macrophages developed a mesenchymal morphology, with numerous protrusions formed at the cell front and an elongated trailing edge (Fig. 6B), comparable to our earlier observations with fixed cells (Fig. 5A).

To assess the influence of RabGTPases in this assay, cells were treated with RabGTPase isoform-specific siRNAs or with luciferase- or MT1-MMP-specific siRNA as controls, cultured for 3 days, and embedded in the collagen plug. After 4 additional days, invading cells were detected by light microscopy (Fig. 6C). Invasive cells present in the outer shell were counted, with control values for luciferase siRNA-treated cells set to 100% (Fig. 6D). Cells treated with MT1-MMP siRNA showed a pronounced reduction in their invasive capacity (20.4±9.4%), consistent with the importance of this protease for mesenchymal invasion (Poincloux et al., 2009). Pronounced reductions of ca. 50% in the number of invasive cells were observed upon knockdown of Rab8a (55.5±19.0% and 51.6±25.3%) and Rab14
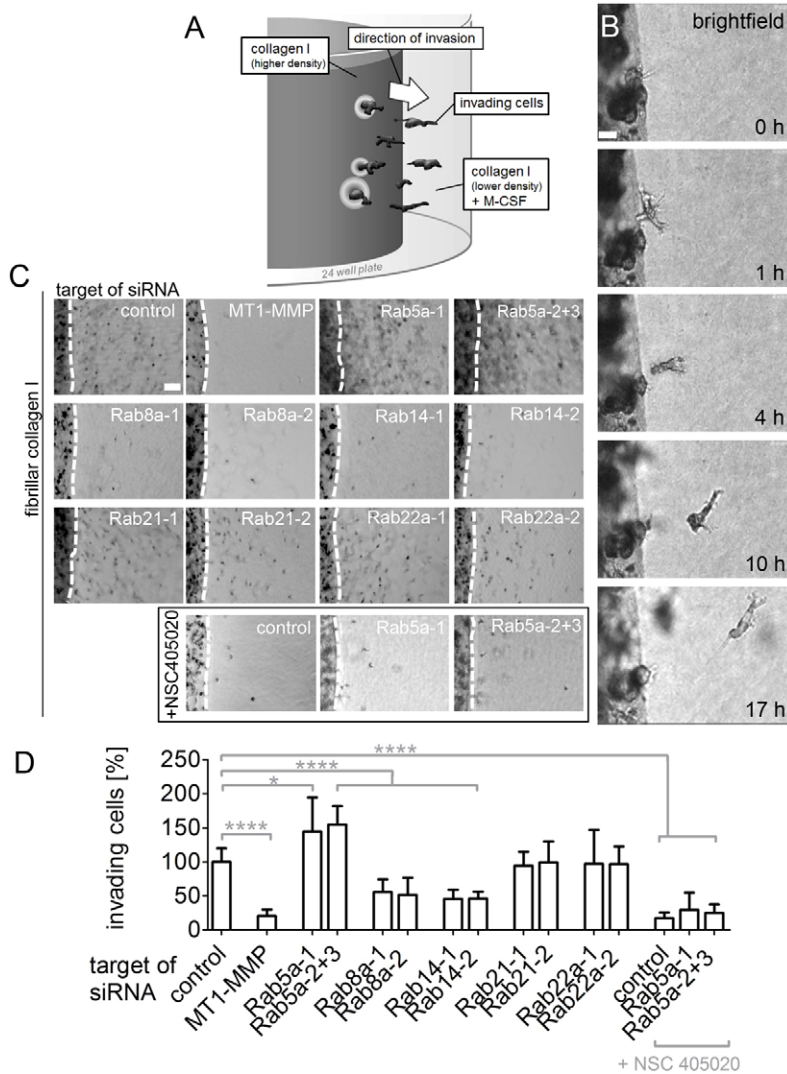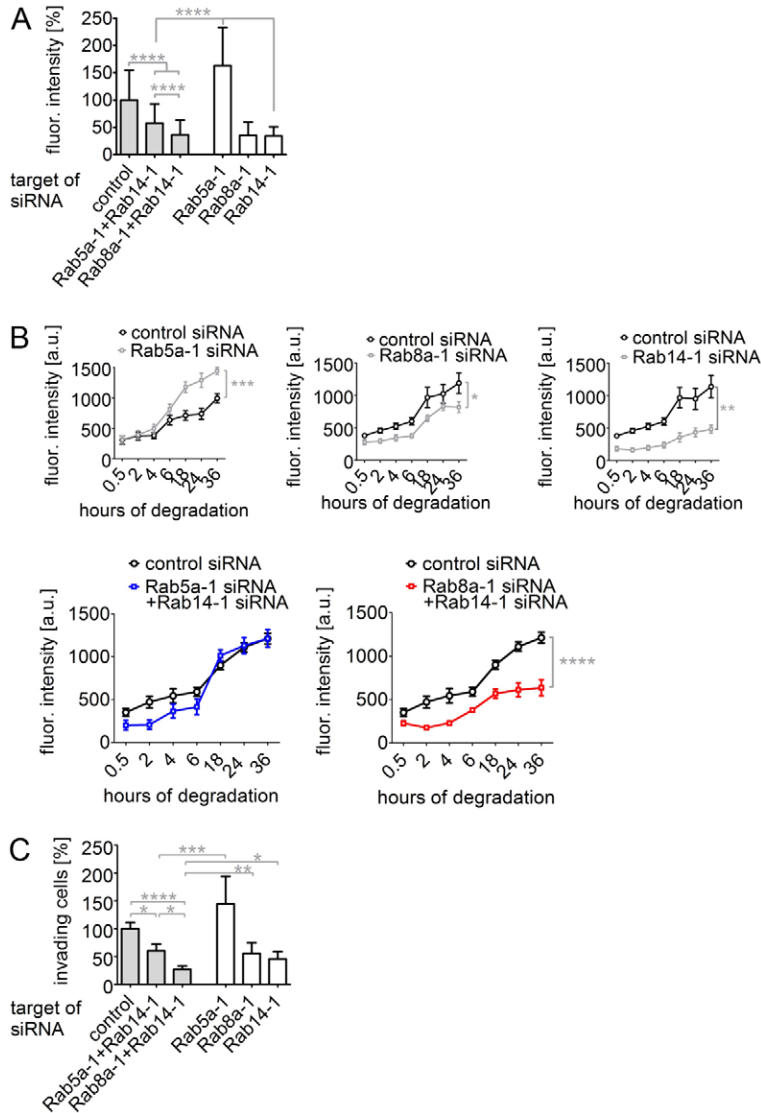
Fig. 6. Knockdown of Rab5a, Rab8a and Rab14, but not of Rab21 and Rab22a, leads to pronounced alterations in 3D invasive behaviour of macrophages. (A) Model of the 3D type I collagen invasion assay. Cells are embedded in a type I collagen plug (2.5 mg/ml) and invade the surrounding shell of less dense type I collagen (2 mg/ml) containing M-CSF as a chemoattractant. (B) Brightfield confocal micrographs of a macrophage invading fibrillar collagen I matrix. Time of image acquisition after start of experiment is indicated. Scale bar: 10 μm. Note dark zone of collagen I with embedded macrophages and brighter zone of surrounding fibrillar collagen I (for experimental set-up, see Materials and Methods), and formation of numerous protrusions of invading macrophage. (C,D) Invasion of macrophages into collagen I matrix. Cells were treated with siRNAs specific for luciferase, as a negative control, MT1-MMP, as a positive control, and for RabGTPase isoforms, and were treated with MT1-MMP inhibitor NSC405020, as indicated. (C) Brightfield micrographs of invading cells. Dashed white lines indicates border between collagen matrix with embedded macrophages and collagen matrix with invaded cells, visible as dark dots. Scale bar: 100 μm for all images. (D) Quantification of cells invading the collagen matrix, at day 4 after seeding. Values for control siRNA were set to 100%. Bars show means + s.d. Asterisks indicate values significantly different from values of control cells: $*P=0.011$, $**P=0.0056$, $***P=0.0001$, $****P<0.0001$. For all values, 16 pictures from three different donors each were evaluated. For specific values, see supplementary material Table S1.

(45.7±13.3% and 46.4±10.1%). By contrast, the levels of invasive cells were unchanged upon knockdown of Rab21 (94.4±20.4% and 99.2±31.1%) and Rab22a (97.1±50.1% and 96.8±26.0%). Strikingly, knockdown of Rab5a resulted in an increased number of invaded cells (144.6±49.7% and 154.7±49.7%). Moreover, use of MT1-MMP inhibitor NSC405020 (1 mM; Remacle et al., 2012) greatly reduced cell invasion (17.1±8.6%; Fig. 6C,D), and this effect could not be rescued by knockdown of Rab5a (29.4±25.5% and 24.7±12.9%; Fig. 6C,D), showing that Rab5a exerts its function in invasion mainly through regulation of MT1-MMP.

To further exclude MT1-MMP-independent effects of RabGTPase knockdown, we tested the viability and ECM binding by performing survival and adhesion assays of cells treated with siRNA specific for MT1-MMP, individual Rab proteins or combinations. Collectively, we find slight variations in the 10–20% range for knockdown of some RabGTPases, including Rab5a, Rab8a and Rab14 (supplementary material Fig. S8). However, considering that all alterations in cell invasion upon knockdown of these Rab proteins are pronounced (±50%; Fig. 6D), the minor, and sometimes even opposing, effects on cell viability or cell adhesion can not explain these effects. The increased invasion in case of Rab5a knockdown and the decreased invasion for Rab8a or Rab14 knockdown cells are thus most likely due to MT1-MMP-associated matrix degradation, and not, or only to a lesser degree, to changes in cell viability or matrix adhesion. We conclude from these results that Rab5a, Rab8a and Rab14 are important regulators of protease-driven mesenchymal invasion in a three-dimensional setting.

Finally, to test how the three identified RabGTPases might work together in MT1-MMP regulation, we measured surface exposure of endogenous MT1-MMP, collagen dequenching in 3D, and invasion into collagen gels, each time under double knockdown of Rab5a and Rab14 or Rab8a and Rab14. Apart from a ca. 10% increase in matrix adhesion for Rab5a/Rab14 double knockdown cells (supplementary material Fig. S8, with values given in supplementary material Table S1), no major alterations were apparent in cells depleted for the specific RabGTPases, ensuring that cell viability and matrix adhesion upon (combined) knockdown of Rab proteins were unchanged. Combined knockdown of Rab5a and Rab14 led to intermediate values in surface exposure of MT1-MMP (57.7±35.3%; Fig. 7A), in 3D collagen dequenching (1213.1±102.6 a.u. at

Fig. 7. Surface exposure of MT1-MMP, collagen I dequenching and 3D invasion of cells with combined knockdown of Rab5a and Rab14 or Rab8a and Rab14. (**A**) Fluorescence intensities of surface-localised endogenous MT1-MMP, based on Alexa Fluor 568 fluorescence. Fluorescence intensities for control siRNA were each set to 100%. For comparison, values for single knockdown of Rab5a, Rab8a and Rab14 are also shown (see also Fig. 3M). For all values, 30 cells from three different donors were evaluated. Graph shows means + s.d.. Asterisks indicate values significantly different from control values: ****$P<0.0001$. For specific values, see supplementary material Table S1. (**B**) Quantification of dequenched collagen I fluorescence in cells treated with indicated siRNAs. In all experiments, two siRNAs against each protein were used (blue and red), and control cells treated with luciferase siRNA were used in parallel (black). Fluorescence intensities are given in arbitrary units (a.u.). Graphs show means + s.e.m. Time after start of experiment is indicated. For comparison, graphs for single knockdown of Rab5a, Rab8a and Rab14 are also shown (see also Fig. 5D). Asterisks indicate values significantly different from control value at 36 h: *$P=0.0143$, **$P=0.0047$, ***$P=0.0003$, ****$P<0.0001$. For all values, 48 measurements from three different donors each were evaluated. For specific values, see supplementary material Table S1. (**C**) Quantification of cells invading collagen I matrix, at day 4 after seeding. Values for control siRNA were set to 100%. For comparison, values for single knockdown of Rab5a, Rab8a and Rab14 are also shown (see also Fig. 6D). Bars show means + s.d. Asterisks indicate values significantly different from values of control cells: *$P<0.0182$, **$P=0.0025$, ***$P=0.0002$, ****$P<0.0001$. For all values, 16 pictures from three different donors each were evaluated. For specific values, see supplementary material Table S1.

36 h; Fig. 7B) and collagen gel invasion (60.3±41.9%; Fig. 7C). Double knockdown of Rab8a and Rab14 led to values similar to those observed for single knockdown of Rab8a in MT1-MMP surface exposure (36.3±26.9%; Fig. 7A) and in 3D collagen dequenching (635.0±91.0 a.u. at 36 h; Fig. 7B), and to even lower values, compared to single knockdowns of either Rab8a or Rab14, in 3D invasion of macrophages (26.7±20.9%; Fig. 7C). We conclude that Rab5a, as a negative regulator of MT1-MMP trafficking, counteracts the effects of Rab14. In contrast, Rab8a and Rab14 are both positive regulators of MT1-MMP trafficking. Moreover, based on their non-additive effects on MT1-MMP cell surface exposure and collagen degradation, Rab8 and Rab14 are likely to regulate common aspects of MT1-MMP trafficking. This is in contrast to their additive effects in the plug invasion assay, suggesting that both Rab proteins regulate separate aspects of cell invasion.

Discussion

A key feature of mesenchymal cell invasion is the ability to proteolytically process extracellular matrix material, which allows cells to transmigrate through a variety of barriers including the endothelial basement membrane (Nourshargh et al., 2010) or interstitial collagen networks (Poincloux et al., 2009). The membrane-bound matrix metalloproteinase MT1-MMP plays a central role in these processes (Poincloux et al., 2009; Wolf and Friedl, 2009; Hotary et al., 2003). Consequently, therapeutic intervention on the level of MT1-MMP activity presents as an attractive option for the potential treatment of invasion-based dysfunctions such as chronic inflammation or metastasis. In order to manipulate MT1-MMP activity in a targeted manner, however, it is vital to understand the molecular mechanisms regulating MT1-MMP activity at the cell surface, which includes trafficking of MT1-MMP vesicles.

RabGTPases are major regulators of intracellular trafficking that act as molecular switches (Stenmark, 2009; Hutagalung and Novick, 2011), with their on/off regulatory function considered to be restricted to the membrane compartments where they are located (Zerial and McBride, 2001). This formed the rationale of our colocalisation screen to identify Rab proteins relevant for MT1-MMP trafficking in macrophages. We found prominent colocalisation of both GFP-fused constructs and endogenous forms of Rab5a, Rab8a, Rab14, Rab21 and Rab22a with

MT1-MMP-positive vesicles. No substantial colocalisation was found for Rab4, Rab6a, Rab9 and Rab11. Our results are consistent with a previous report showing localisation of Rab8, but not Rab11, on MT1-MMP vesicles in MDA-MB-231 adenocarcinoma cells (Bravo-Cordero et al., 2007). At the same time, these data do not exclude the possibility that other members of the extensive Rab family might also colocalise with MT1-MMP and regulate MT1-MMP functions in macrophages. Still, control experiments using dominant active/negative constructs and siRNA-mediated knockdown (supplementary material Fig. S6D) for Rab6a show that, at least for this isoform, absence of localisation to MT1-MMP vesicles is coupled to absence of a regulatory influence on MT1-MMP-dependent parameters such as surface exposure, 3D matrix degradation and 3D invasion (supplementary material Fig. S9).

Besides colocalisation with MT1-MMP vesicles, we also observed the formation of enlarged vesicles or tubules upon overexpression of Rab5a, Rab14, Rab21 and Rab22a wt constructs. Similar observations of 'giant vesicles' have been reported upon overexpression of DA Rab5 in BHK and HeLa cells (Stenmark et al., 1994), for both wt and DA Rab14 in NRK rat kidney cells (Junutula et al., 2004), of wt Rab21 in MDA-MB-231 breast cancer cells (Pellinen et al., 2006) and of wt Rab22 in BHK cells (Olkkonen et al., 1993). While this phenomenon represents an artefact of enhanced RabGTPase activity, the enlarged surface of these structures revealed that RabGTPases and MT1-MMP–mCherry often localised to distinct domains at the membrane. The common localisation to a vesicle subpopulation does, therefore, not imply colocalisation or even interaction of these proteins. These findings are also consistent with reports that RabGTPases are not randomly distributed on organelles, but are clustered in functional domains (Zerial and McBride, 2001; Sönnichsen et al., 2000).

In order to assess the relevance of the identified RabGTPases for MT1-MMP trafficking, we next determined their impact on their regulation of MT1-MMP pools at the cell surface. Out of five RabGTPases (Rab5a, Ra8a, Rab14, Rab21, Rab22a) showing prominent colocalisation with MT1-MMP-positive vesicles, four isoforms (Rab5a, Rab8a, Rab14, Rab22a) had a significant impact on the cell surface exposure of MT1-MMP, with Rab5a emerging as a negative regulator, and Rab8a, Rab14 and Rab22a as positive regulators of MT1-MMP cell surface exposure. This is in line with the key role of Rab5 during membrane fusion in endocytosis (Stenmark, 2009; Stenmark et al., 1994), and also of the Rab5 effector EEA-1 in the early endosome tethering and docking (Christoforidis et al., 1999). Rab8a has already been identified as a regulator of MT1-MMP exocytosis in MDA-MB-231 cells (Bravo-Cordero et al., 2007), and our results confirm this role for primary human macrophages, pointing to a probably general role of Rab8 in MT1-MMP exocytosis. The detected role for Rab14 in MT1-MMP surface exposure appears to be consistent with the localisation of Rab14 on early endosomes and the observed defects in transferrin recycling upon depletion of Rab14 (Yamamoto et al., 2010). Rab21 activity is clearly not required for MT1-MMP trafficking in macrophages. However, localisation of Rab21 at early endosomes, which are also positive for Rab5a (Simpson et al., 2004) may explain its localisation at MT1-MMP vesicles in this study. Rab22 also shows localisation at early endosomes (Kauppi et al., 2002) and has been implicated in the recycling of membrane proteins that are internalised independently of clathrin (Chen et al., 1994). This seems to be consistent with the finding

that surface-localised MT1-MMP can be internalised by both clathrin-dependent and -independent pathways (Remacle et al., 2003). Moreover, Rab4 and Rab11, which both regulate recycling of clathrin-dependent cargo (Schlierf et al., 2000; van der Sluijs et al., 2001), did not colocalise with MT1-MMP in the screen. This suggests that uptake of MT1-MMP from the cell surface proceeds mostly via clathrin-independent pathways in primary macrophages.

Collectively, these data point to the following possible scenario of Rab-dependent trafficking of MT1-MMP in macrophages (Fig. 8): surface-associated MT1-MMP is taken up by endocytosis, which is controlled by Rab5a. Substantial parts of this pool are recycled back to the cell surface, through processes controlled by Rab14 and Rab22a, which probably reflects their respective roles in the slow and fast recycling routes for re-internalised surface proteins (Sönnichsen et al., 2000; Yudowski et al., 2009). Rab8a impacts on MT1-MMP trafficking by regulating the biosynthetic pathway from the Golgi, which can proceed via exocytic vesicles or recycling endosomes (Henry and Sheff, 2008; Grant and Donaldson, 2009). In addition, eventual degradation by lysosomes is expected to occur, to balance synthesis of new material. This model is further substantiated by our experiments using double knockdown cells. Combined knockdown of Rab5a and Rab14 led to intermediate values in surface exposure of MT1-MMP, in 3D collagen dequenching and collagen gel invasion, arguing for opposing roles of these RabGTPases in MT1-MMP trafficking, which would be
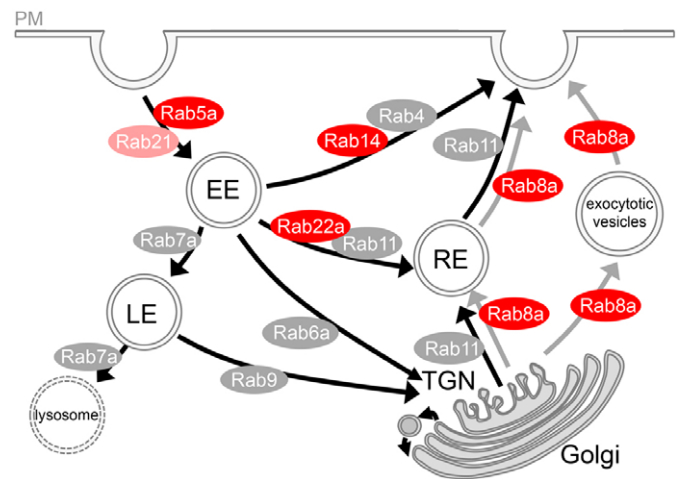
Fig. 8. Model of MT1-MMP trafficking in macrophages. Surface-associated MT1-MMP is taken up by endocytosis, which is controlled by Rab5a. Parts of this pool are recycled back to the cell surface, either by fast recycling controlled by Rab14 or by slow recycling through recycling endosomes controlled by Rab22a. Trafficking of newly synthesized MT1-MMP to the cell surface is controlled by Rab8a and may occur by exocytotic vesicles or recycling endosomes. RabGTPase isoforms colocalising with MT1-MMP in macrophages are indicated at their respective compartments. RabGTPases that are major regulators of MT1-MMP-dependent cell invasion in 3D are highlighted in deep red (Rab21, colocalising with MT1-MMP vesicles, but without major impact on MT1-MMP trafficking, in light red; other major RabGTPases, including tested isoforms without impact on recycling or biosynthetic trafficking of MT1-MMP in grey). EE, early endosomes; LE, late endosomes; RE, recycling; PRE, perinuclear recycling endosomes; TGN, trans-Golgi network. The plasma membrane is indicated as a double line.

Table 1. Overview for MT1-MMP distribution after various treatments

	Alteration of MT1-MMP distribution*								
	Target of siRNA/GFP–Rab DN overexpression								
Assay	Rab4	Rab5a	Rab6a	Rab8a	Rab9	Rab11	Rab14	Rab21	Rab22a
Colocalisation with MT-MMP	−	+	−	+	−	−	+	+	+
Surface exposure	n.a.	↑ ↑	↔	↓ ↓	n.a.	n.a.	↓ ↓	↔	↓ ↓
Recruitment to podosomes	n.a.	↑ ↑	n.a.	↓ ↓	n.a.	n.a.	↓ ↓	↔	↓ ↓
Matrix degradation on 2D gelatin	n.a.	↑ ↑	n.a.	↓ ↓	n.a.	n.a.	↓ ↓	↔	↓ ↓
Matrix degradation in 3D collagen I	n.a.	↑	↔	↓	n.a.	n.a.	↓ ↓	↔	↓ ↓
Invasion into 3D collagen I	n.a.	↑ ↑	↔	↓ ↓	n.a.	n.a.	↓ ↓	↓	↔

*Compared with adequate control cells.
−, negative.
+, positive.
(↑) ↑, (pronounced) increase.
(↓) ↓, (pronounced) decrease.
↔, no significant change.
n.a., not analysed.

consistent with roles for Rab5a in endocytosis and for Rab14 in exocytosis of MT1-MMP. Moreover, combined knockdown of Rab8a and Rab14 led to values similar to those observed for single knockdown of Rab14 in MT1-MMP surface exposure and in 3D collagen dequenching. This non-additive effect suggests that both Rab proteins address aspects of the same pathway that regulates MT1-MMP trafficking and proteolytic activity. The additive effect of their combined knockdown in 3D collagen invasion further suggests that Rab8 and Rab14 have only partially overlapping functions in cell invasion. This might reflect regulation not only of MT1-MMP trafficking during proteolytic invasion, but also of other aspects such as adhesion or de-adhesion.

To test the significance of the identified Rab proteins for MT1-MMP-dependent functions, we also analysed their impact on matrix degradation by primary macrophages in both 2D and 3D settings. Podosomes are actin-rich cell-matrix contacts, that have emerged as central structures mediating matrix degradation and cell invasion (Murphy and Courtneidge, 2011; Linder, 2007), especially by monocytic cells including macrophages (Linder et al., 1999), dendritic cells (Burns et al., 2001) and osteoclasts (Destaing et al., 2003). Podosomes are able to degrade matrix material by localised release of ECM-lytic factors, including proteinases of the matrix metalloproteinase family (Wiesner et al., 2010; Delaissé et al., 2003; Tatin et al., 2006), and especially MT1-MMP has been shown to be crucial for podosome-localised ECM degradation (Linder, 2007). Indeed, microtubule plus ends have been shown to contact podosomes (Kopp et al., 2006), which is consistent with microtubule-dependent trafficking of MT1-MMP to these structures (Wiesner et al., 2010).

We now find that knockdown of Rab5a leads to enhanced contact events of MT1-MMP–mCherry vesicles with podosomes, while knockdown of Rab8a, Rab14 and Rab22a results in a reduction of contact events. These results correlate well with respective changes upon RabGTPase knockdown in the matrix degradation assay and point to Rab5a, Rab8a, Rab14 and Rab22a as important regulators of matrix degradation in macrophages, most probably by mediating the vesicular delivery of the key proteinase MT1-MMP to the main degradative structures of these cells. Direct involvement of RabGTPases in MT1-MMP-mediated ECM degrading processes has so far only been reported for Rab8, which has been shown to regulate collagen degradation by MDA-MB-231 cells (Bravo-Cordero et al., 2007). Our results confirm this role now also for gelatin degradation by primary macrophages. The only other Rab isoforms implicated in matrix degradation is Rab4a, which is involved in procathepsin L secretion in human melanoma cells (Barbarin and Frade, 2011). However, MT1-MMP does not localise to Rab4-positive vesicles in human macrophages.

It is important to consider that cell culture on 2D matrices creates a polarisation of the cell, resulting in basal and apical surfaces. This is useful for the experimental study of different outputs such as apical surface exposure of MT1-MMP or matrix degradation at the basal cell side. Moreover, it is most probably also a relevant process *in vivo*, as invasive cells do encounter two-dimensional barriers, including contact of monocytic cells with the endothelium or attachment of osteoclasts to bone surfaces (Linder et al., 2011). Within tissues, however, cells are surrounded by a three-dimensional environment, which is expected to influence both regulatory pathways involved in matrix degradation as well as the matrix-degrading organelles themselves. Indeed, primary human macrophages in gelled collagen I matrix have been shown to form long, dynamic protrusions that are enriched at their tips in podosome components such as F-actin, cortactin, talin, vinculin and CD44 (Van Goethem et al., 2010; Vérollet et al., 2011). Colocalisation of these structures with matrix defects and also with fluorescence signals in the collagen dequenching assay support the idea that these structures exhibit degradative capacity (Van Goethem et al., 2010). This is further underlined by our finding that these tip structures are also enriched in MT1-MMP. Collectively, these structures, (1) possess the typical composition of podosomes, if arranged in a different architecture, (2) recruit the major matrix-degrading protease MT1-MMP, and (3) colocalise with sites of matrix degradation, which qualifies them as bone fide 3D equivalents of 2D podosomes.

Of note, 3D invasion is a complex multi-step process involving adhesion to matrix, proteolytic cleavage of matrix components, as well as de-adhesion and pulling of the cell body (Friedl and Wolf, 2009). The impact of the identified Rab proteins on this process may thus not only reflect MT1-MMP dependent matrix degradation, but may also involve other MT1-MMP functions such as integrin processing at the cell surface (Barbolina and Stack, 2008) or cleavage of matrix receptors such as syndecan-1

(Endo et al., 2003; Wiesner et al., 2010). The complex nature of cell invasion may also explain the different influence of Rab5 on invasion of macrophages and cancer cells. In HeLa and human cervical carcinoma cells, Rab5a positively regulates focal adhesion formation (Liu et al., 2011). Decreased invasion of these cells is thus likely based on defects in cell de-/adhesion. In contrast, Rab5 negatively influences matrix degradation in primary macrophages, which transmits as a negative influence on 3D invasion of these cells. The influence of Rab5a particularly on MT1-MMP in macrophages is also evident from experiments using the MT1-MMP inhibitor NSC405020 in the 3D cell invasion assay. Here, use of NSC405020 completely reverted the invasion-promoting effect of Rab5a knockdown and decreased it to control levels (Fig. 6D), demonstrating that Rab5a exerts its function in macrophage invasion mainly through MT1-MMP.

Different functions of surface-associated MT1-MMP may be differentially influenced by the recycling route the protease takes within cells, which could offer an explanation why Rab22a, which is involved in regulating the surface pool of MT1-MMP, has no apparent impact on 3D invasion of macrophages, in contrast to Rab8a and Rab14. Indeed, the potential association of different pools of MT1-MMP with distinct intracellular trafficking routes has been speculated upon earlier (Schlierf et al., 2000). Of course, this does not exclude that Rab-dependent trafficking of other cargo molecules, for example integrins or other metalloproteinases such as ADAMs, impact on 3D invasion of macrophages. However, we consistently found, (1) strong functional correlation between inhibition of specific Rab isoforms and knockdown of MT1-MMP, (2) Rab14, which regulates ADAM10 trafficking in epithelial cells (Linford et al., 2012), does not colocalise with MT1-MMP vesicles in macrophages, and (3) Rab4, Rab11 and Rab21, major regulatory Rabs for integrin trafficking (Pellinen et al., 2006; Caswell et al., 2009), showed no pronounced influence on MT1-MMP trafficking or function in this study.

Collectively, our data identify three specific RabGTPases, Rab5a, Rab8a and Rab14, as major regulators of MT1-MMP trafficking and function in primary human macrophages. We show that these RabGTPases control the pericellular activity of MT1-MMP by regulating the cell surface exposure of MT1-MMP, modulating contact of MT1-MMP-positive vesicles with podosomes and thus impact on extracellular matrix degradation and ultimately on proteolytic invasion of macrophages. At the same time, our results show that the relevance of potential MT1-MMP regulators should be tested in a variety of experimental set ups, and that neither colocalisation nor influence on matrix degradation in 2D alone is sufficient to correctly predict an influence on proteolytic cell invasion in 3D. This appears to be consistent with recent findings in breast cancer cells that many parameters of 2D migration have only limited prognostic value for 3D invasion (Meyer et al., 2012).

Alterations in RabGTPase expression or activity can cause defects in cell adhesion, motility and invasion, leading to neurologic diseases, lipid storage disorders or cancer (Agola et al., 2011). Accordingly, Rab5a is hyperactivated in lung adenocarcinoma (Stein et al., 2003), Rab5 and Rab8 have been implicated in Parkinson's disease by affecting α-synuclein transport (Gitler et al., 2008), and Rab22a is upregulated in hepatocellular carcinoma (Agola et al., 2011). Consequently, these RabGTPases are being considered as target molecules for therapeutic intervention (Stein et al., 2003). Our results now implicate Rab5a, Rab8a and Rab14 as potential targets for therapeutic modulation of macrophage invasion and may thus indicate alternative, if challenging, routes for the treatment of invasion-based immune cell dysfunctions.

Material and Methods

Cell preparation, culture and transfection
Human peripheral blood monocytes were isolated from buffy coats and differentiated into macrophages, as described previously (Kopp et al., 2006). Cells were cultured in RPMI containing 20% autologous serum at 37°C, 5% CO_2 and 90% humidity. Transient transfections were performed using the Neon® Transfection System (Life technologies, Invitrogen, Darmstadt, Germany) with standard settings (1000 V, 40 ms, 2 pulses) and appropriate amounts of siRNA (650 ng) and plasmids (0.5–1.5 µg/10 000 cells), respectively.

Antibodies and constructs
Mouse monoclonal antibody (mAb) anti-MT1-MMP and anti-α actin were purchased from Millipore (Billerica, MA), rabbit mAb anti-Rab5 from Cell Signaling (Danvers, MA), mouse mAb anti-Rab8 (used for immunoblotting) from BD (Franklin Lakes, NJ), rabbit polyclonal antibody (pAb) anti-Rab8a (used for immunostaining) from Sigma (St. Louis, MO), rabbit pAb anti-Rab14 from Abcam (Cambridge, UK) and rabbit pAb anti-Rab22a from ProteinTech (Group, Chicago, IL). Rabbit pAb anti-Rab21 was a kind gift from J. Fransen (University of Nijmegen, Netherlands). mCherry antibody was kindly provided by J. Faix (Hannover medical school, Germany). Collagen 3/4 antibody was a kind gift from P. Friedl (Radboud University Nijmegen, Netherlands). All fluorochrome-conjugated secondary antibodies were purchased from Molecular Probes (Eugene, OR). MT1-MMP-mCherry was kindly provided by P. Chavrier (Institute Curie, Paris, France); pGreenlantern-Rab5wt (wild type), pGreenlantern-Rab5 S34N (dominant negative, DN) and pGreenlantern-Rab5 Q79L (dominant active, DA) were generously provided by Craig Roy (Yale University, New Haven, CT); GFP-Rab6awt, GFP-Rab6a Q72L (DA) and GFP-Rab6a T27N (DN) were kind gifts from J. Kremerskothen (University Hospital Muenster, Germany); GFP-Rab8wt, GFP-Rab8aQ67L (DA) and GFP-Rab8aT22N (DN) were kindly provided by D. Sheff (Carver College of Medicine, Iowa City, IA); GFP-Rab14wt, GFP-Rab14 S25N (DN) and GFP-Rab14 Q70L (DA) were gifts from R. H. Scheller (Genentech Inc., San Francisco, CA), GFP-Rab21wt, GFP-Rab21 T33N (DN), GFP-Rab21 Q78L (DA) were gifts from J.C. Simpson (University College Dublin, Ireland), GFP-Rab22awt, GFP-Rab22a S19N (DN), GFP-Rab22a Q64L (DA) were gifts from J. Donaldson (National Institutes of Health, Bethesda, MD).

Microscopy
Images of fixed samples were acquired with a confocal laser-scanning microscope (Leica DM IRE2 with a Leica TCS SP2 AOBS confocal point scanner) equipped with an oil-immersion HCX PL APO 63× NA 1.4 λ_{blue} objective. Detailed fluorescence images of cells in 3D collagen were acquired with a confocal laser-scanning microscope (Leica DMI 6000 with a Leica TCS SP5 AOBS confocal point scanner) equipped with a water-immersion HCX PL APO 63× NA 1.4-0.6 objective.

Immunoblotting
Immunolabelling was performed by standard procedure (Kopp et al., 2006), using the above mentioned anti-MT1-MMP, Rab5, Rab8, Rab14, Rab21, Rab22a, or α-actin antibodies and horseradish peroxidase-coupled anti-mouse or anti-rabbit IgG (Dianova, Hamburg, Germany) as secondary antibodies. Protein bands were visualised by using Super Signal kit (Pierce Chemical, Rockford, IL) and X-Omat AR film (Kodak, Stuttgart, Germany).

Live cell imaging
Images were acquired with a spinning disc confocal system (Spinning disc CSU22, Yokogawa, Japan) fitted on a Zeiss Axiovert 200M microscope with a temperature- and CO_2-controllable environmental chamber (Solent Scientific, Regensworth, UK), oil immersion Plan-Apo 63× NA 1.4 objective and a CCD camera (EM-CCD C-9100-2, Hamamatsu, Japan). Acquisition and processing of images was performed with Volocity Software (Improvision, Coventry, UK). Cells were seeded on glass-bottomed dishes (ibidi) at a density of 2×10^5 and incubated for 20 h before the start of the experiment.

SiRNA-induced knockdown
Specific targeting duplex siRNA were generated (MWG, Ebersberg, Germany) as follows: 5′-AACCAGGAATCAGTGTTGTAG-3′ (Rab5a-1); 5′-AAGCACAGT-CCTATGCAGATG-3′ (Rab5a-2) and 5′-GAAGAGGAGTAGACCTTAC-3′ (Rab5a-3); 5′-GACATCTTTGATCACCAGA-3′ (Rab6a-1); 5′-CACCTA-TCAGGCAACAATT-3′ (Rab6a-2); 5′-AAGAGACAAGTTTCCAAGGAA-3′

(Rab8a-1); 5′-CGCATTTTTCACTCTCGCC-3′ (Rab8a-2); 5′-AAGGAAT-CTCACCAATCCAAA-3′ (Rab14-1); 5′-AAGAAGTACATATAACCACTT-3′ (Rab14-2); 5′-AAGTTTAACGACAAGCACATC-3′ (Rab21-1); 5′-AAGAGA-GATTCCATGCATTGG-3′ (Rab21-2); 5′-AAGGACTACGCCGACTCTATT-3′ (Rab22a-1); 5′-CTGCAGCTATAATCGTTT ATG-3′ (Rab22a-2); 5′-AACA-GGCAAGCGTGATGCAGA-3′ (MT1-MMP); firefly luciferase targeting siRNA 5′-AGGTAGTGTAACCGCCTTGTT-3′ was used as negative control. MT1-MMP siRNA was tested in primary human macrophages and led to a reduction of ca. 95% 3 days after transfection.[24] Primary human macrophages were transfected with siRNA (650 ng) twice at 0 h and 48 h, and evaluated after a further incubation period of 18 h.

Cell survival assay
Cells were transfected with siRNA twice at 0 h and 48 h. On day 7 after initial transfection, cell survival was determined by staining the cells with Crystal Violet (5 mg/ml), resolving the stain with 2% SDS, and measuring the absorbance at 550 nm. For each value, nine points evenly distributed within one well of a 96-well plate were measured. In total, triplicates from three different donors were evaluated. Mean value of control cells was set as 100%. Statistical analysis was performed with Microsoft Excel and GraphPad Prism software. For specific values, see supplementary material Table S1.

Cell adhesion to ECM assay (Collagen I)
Cells were transfected with siRNA twice at 0 h and 48 h. On day 7, cells were detached and left to adhere for 20 min in a 96-well plate, coated with collagen I (Biochrome AG, Berlin, Germany). Cell adherence was determined as described previously (Humphries, 2009) using Crystal Violet as used to determine the survival of the cells. For each value, nine points evenly distributed within one well of a 96-well plate were measured. In total, triplicates from three different cell donors were evaluated. Mean value of control cells was set as 100%. Statistical analysis was performed with Microsoft Excel and GraphPad Prism software. For specific values, see supplementary material Table S1.

Surface exposure of MT1-MMP
Macrophages were seeded on non-coated glass coverslips in a density of 1×10^5, or seeded in Collagen I (2.5 μg/ml; from rat tail, Becton Dickinson), fixed with 3.7% formaldehyde solution, but not permeabilised. Surface MT1-MMP–mCherry and endogenous surface MT1-MMP was stained with specific antibodies (anti-mCherry and anti-MT1-MMP, respectively), followed by Cy5- and Alexa-Fluor-568-conjugated secondary antibodies, respectively, as also described previously (Wiesner et al., 2010). Quantification of Cy5- or Alexa-Fluor-568-based fluorescence intensity was performed using ImageJ software for measurement of the cell surface exposure of MT1-MMP. In the case of overexpressed MT1-MMP, values of surface-exposed MT1-MMP–mCherry were set relative to values of total overexpressed MT1-MMP–mCherry for normalisation. Values of control cells were set to 100%. For comparability, laser intensity was not changed between measurements. For each value, 3×30 cells were evaluated. Statistical analysis was performed with Microsoft Excel and GraphPad Prism software. When indicated, differences between mean values were analysed using the Student's t-test.

2D gelatin degradation assay
Gelatin (from swine, Roth, Karlsruhe, Germany) was fluorescently labelled with NHS-Rhodamine (ThermoScientific, Rockford, IL), according to (Chen et al., 1994). Coverslips were coated with labelled matrix solution, fixed in 0.5% glutaraldehyde (Roth) and washed with 70% ethanol and medium. Cells were seeded on coated coverslips with a density of 8×10^4, fixed and permeablised 6 h post seeding and stained with Alexa-Fluor-647-conjugated phalloidin. Values of matrix degradation were determined by a loss of fluorescence intensity relatively to non-degraded matrix, using ImageJ software. Values of control cells were set to 100%. For comparability, laser intensity was not changed between measurements. For each value, 3×30 cells were evaluated. Values were analysed using Windows Excel software. Statistical analysis was performed with GraphPad Prism software. When indicated, differences between mean values were analysed using the Student's t-test.

3D collagen i degradation assay
To measure 3D collagen I matrix degradation, primary human macrophages were copolymerised with rat tail collagen (2.5 mg/ml; Becton Dickinson), containing 2% quenched DQ^{TM} collagen I (fluorescein conjugated, from bovine skin, Molecular Probes). Emitted light was measured and quantified by spectrofluorometry at a wavelength of 530 nm. Background fluorescence was analysed by measuring the fluorescence intensity of matrix without cells. For each value, 16 points evenly distributed within one well of a 96-well plate were measured; in total, three wells from three different cell donors were evaluated ($n=144$). Statistical analysis was performed with GraphPad Prism software. When indicated, differences between mean values over the whole time of measurement were analysed using the Student's t-test.

3D collagen i invasion assay
To measure invasive capacity of cells into a 3D collagen I matrix, primary human macrophages were copolymerised with rat tail collagen (2.5 mg/ml; Becton Dickinson) and embedded in rat tail collagen I (2 mg/ml) containing 10 ng/ml Macrophage-Colony Stimulating Factor (M-CSF, Relia Tech, Wolfenbüttel, Germany). When indicated, MT1-MMP inhibitor (NSC405020, 1 mM, Millipore) was added to the collagen I prior to polymerisation. The lower concentration of collagen I in the outer gel (2 mg/ml) was chosen to facilitate invasion outwards from the inner plug. This was based on initial testing of several different combinations of collagen concentrations for inner and outer gels. The one presented here is the one that allowed invasion in principal but hindered it under knockdown of MT1-MMP. M-CSF was chosen as a known chemoattractant for macrophages (Pixley, 2012). We found that addition of M-CSF to the outer gel enhances the number of outwardly invading cells approximately twofold (supplementary material Fig. S10A,B), without influencing cell viability (supplementary material Fig. S10C) and thus provides a clearer readout of cell invasion. The number of cells that invaded the surrounding matrix was counted after 4 days of invasion, using ImageJ cell counter. Four wells per donor and three donors in total were analysed ($n=16$). Statistical analysis was performed with GraphPad Prism software. When indicated, differences between mean values of measurement were analysed using the Student's t-test.

Author Contributions
C.W. designed and performed experiments as part of the doctoral thesis, K.A. performed experiments, and S.L. designed experiments and wrote the manuscript.

Supplementary material available online at
http://jcs.biologists.org/lookup/suppl/doi:10.1242/jcs.122358/-/DC1

References
Agola, J. O., Jim, P. A., Ward, H. H., Basuray, S. and Wandinger-Ness, A. (2011). Rab GTPases as regulators of endocytosis, targets of disease and therapeutic opportunities. *Clin. Genet.* **80**, 305-318.

Barbarin, A. and Frade, R. (2011). Procathepsin L secretion, which triggers tumour progression, is regulated by Rab4a in human melanoma cells. *Biochem. J.* **437**, 97-107.

Barbolina, M. V. and Stack, M. S. (2008). Membrane type 1-matrix metalloproteinase: substrate diversity in pericellular proteolysis. *Semin. Cell Dev. Biol.* **19**, 24-33.

Bravo-Cordero, J. J., Marrero-Diaz, R., Megías, D., Genís, L., García-Grande, A., García, M. A., Arroyo, A. G. and Montoya, M. C. (2007). MT1-MMP proinvasive activity is regulated by a novel Rab8-dependent exocytic pathway. *EMBO J.* **26**, 1499-1510.

Bravo-Cordero, J. J., Hodgson, L. and Condeelis, J. (2012). Directed cell invasion and migration during metastasis. *Curr. Opin. Cell Biol.* **24**, 277-283.

Burns, S., Thrasher, A. J., Blundell, M. P., Machesky, L. and Jones, G. E. (2001). Configuration of human dendritic cell cytoskeleton by Rho GTPases, the WAS protein, and differentiation. *Blood* **98**, 1142-1149.

Caswell, P. T., Vadrevu, S. and Norman, J. C. (2009). Integrins: masters and slaves of endocytic transport. *Nat. Rev. Mol. Cell Biol.* **10**, 843-853.

Chen, W. T., Yeh, Y. and Nakahara, H. (1994). An in vitro cell invasion assay: determination of cell surface proteolytic activity that degrades extracellular matrix. *J. Tissue Cult. Methods* **16**, 177-181.

Christoforidis, S., McBride, H. M., Burgoyne, R. D. and Zerial, M. (1999). The Rab5 effector EEA1 is a core component of endosome docking. *Nature* **397**, 621-625.

Delaissé, J. M., Andersen, T. L., Engsig, M. T., Henriksen, K., Troen, T. and Blavier, L. (2003). Matrix metalloproteinases (MMP) and cathepsin K contribute differently to osteoclastic activities. *Microsc. Res. Tech.* **61**, 504-513.

Destaing, O., Saltel, F., Géminard, J. C., Jurdic, P. and Bard, F. (2003). Podosomes display actin turnover and dynamic self-organization in osteoclasts expressing actin-green fluorescent protein. *Mol. Biol. Cell* **14**, 407-416.

Endo, K., Takino, T., Miyamori, H., Kinsen, H., Yoshizaki, T., Furukawa, M. and Sato, H. (2003). Cleavage of syndecan-1 by membrane type matrix metalloproteinase-1 stimulates cell migration. *J. Biol. Chem.* **278**, 40764-40770.

Friedl, P. and Wolf, K. (2003). Tumour-cell invasion and migration: diversity and escape mechanisms. *Nat. Rev. Cancer* **3**, 362-374.

Friedl, P. and Wolf, K. (2008). Tube travel: the role of proteases in individual and collective cancer cell invasion. *Cancer Res.* **68**, 7247-7249.

Friedl, P. and Wolf, K. (2009). Proteolytic interstitial cell migration: a five-step process. *Cancer Metastasis Rev.* **28**, 129-135.

Frittoli, E., Palamidessi, A., Disanza, A. and Scita, G. (2011). Secretory and endo/exocytic trafficking in invadopodia formation: the MT1-MMP paradigm. *Eur. J. Cell Biol.* **90**, 108-114.

Gitler, A. D., Bevis, B. J., Shorter, J., Strathearn, K. E., Hamamichi, S., Su, L. J., Caldwell, K. A., Caldwell, G. A., Rochet, J. C., McCaffery, J. M. et al. (2008). The Parkinson's disease protein alpha-synuclein disrupts cellular Rab homeostasis. *Proc. Natl. Acad. Sci. USA* **105**, 145-150.

Grant, B. D. and Donaldson, J. G. (2009). Pathways and mechanisms of endocytic recycling. *Nat. Rev. Mol. Cell Biol.* **10**, 597-608.

Guiet, R., Van Goethem, E., Cougoule, C., Balor, S., Valette, A., Al Saati, T., Lowell, C. A., Le Cabec, V. and Maridonneau-Parini, I. (2011). The process of macrophage migration promotes matrix metalloproteinase-independent invasion by tumor cells. *J. Immunol.* **187**, 3806-3814.

Henry, L. and Sheff, D. R. (2008). Rab8 regulates basolateral secretory, but not recycling, traffic at the recycling endosome. *Mol. Biol. Cell* **19**, 2059-2068.

Hotary, K. B., Allen, E. D., Brooks, P. C., Datta, N. S., Long, M. W. and Weiss, S. J. (2003). Membrane type I matrix metalloproteinase usurps tumor growth control imposed by the three-dimensional extracellular matrix. *Cell* **114**, 33-45.

Humphries, M. J. (2009). Cell adhesion assays. *Methods Mol. Biol.* **522**, 203-210.

Hutagalung, A. H. and Novick, P. J. (2011). Role of Rab GTPases in membrane traffic and cell physiology. *Physiol. Rev.* **91**, 119-149.

Itoh, Y. and Seiki, M. (2004). MT1-MMP: an enzyme with multidimensional regulation. *Trends Biochem. Sci.* **29**, 285-289.

Junutula, J. R., De Maziére, A. M., Peden, A. A., Ervin, K. E., Advani, R. J., van Dijk, S. M., Klumperman, J. and Scheller, R. H. (2004). Rab14 is involved in membrane trafficking between the Golgi complex and endosomes. *Mol. Biol. Cell* **15**, 2218-2229.

Kajita, M., Itoh, Y., Chiba, T., Mori, H., Okada, A., Kinoh, H. and Seiki, M. (2001). Membrane-type 1 matrix metalloproteinase cleaves CD44 and promotes cell migration. *J. Cell Biol.* **153**, 893-904.

Kauppi, M., Simonsen, A., Bremnes, B., Vieira, A., Callaghan, J., Stenmark, H. and Olkkonen, V. M. (2002). The small GTPase Rab22 interacts with EEA1 and controls endosomal membrane trafficking. *J. Cell Sci.* **115**, 899-911.

Kopp, P., Lammers, R., Aepfelbacher, M., Woehlke, G., Rudel, T., Machuy, N., Steffen, W. and Linder, S. (2006). The kinesin KIF1C and microtubule plus ends regulate podosome dynamics in macrophages. *Mol. Biol. Cell* **17**, 2811-2823.

Lämmermann, T. and Sixt, M. (2009). Mechanical modes of 'amoeboid' cell migration. *Curr. Opin. Cell Biol.* **21**, 636-644.

Lehti, K., Lohi, J., Valtanen, H. and Keski-Oja, J. (1998). Proteolytic processing of membrane-type-1 matrix metalloproteinase is associated with gelatinase A activation at the cell surface. *Biochem. J.* **334**, 345-353.

Ley, K., Laudanna, C., Cybulsky, M. I. and Nourshargh, S. (2007). Getting to the site of inflammation: the leukocyte adhesion cascade updated. *Nat. Rev. Immunol.* **7**, 678-689.

Linder, S. (2007). The matrix corroded: podosomes and invadopodia in extracellular matrix degradation. *Trends Cell Biol.* **17**, 107-117.

Linder, S., Nelson, D., Weiss, M. and Aepfelbacher, M. (1999). Wiskott-Aldrich syndrome protein regulates podosomes in primary human macrophages. *Proc. Natl. Acad. Sci. USA* **96**, 9648-9653.

Linder, S., Wiesner, C. and Himmel, M. (2011). Degrading devices: invadosomes in proteolytic cell invasion. *Annu. Rev. Cell Dev. Biol.* **27**, 185-211.

Linford, A., Yoshimura, S., Nunes Bastos, R., Langemeyer, L., Gerondopoulos, A., Rigden, D. J. and Barr, F. A. (2012). Rab14 and its exchange factor FAM116 link endocytic recycling and adherens junction stability in migrating cells. *Dev. Cell* **22**, 952-966.

Liu, S. S., Chen, X. M., Zheng, H. X., Shi, S. L. and Li, Y. (2011). Knockdown of Rab5a expression decreases cancer cell motility and invasion through integrin-mediated signaling pathway. *J. Biomed. Sci.* **18**, 58.

Matías-Román, S., Gálvez, B. G., Genís, L., Yáñez-Mó, M., de la Rosa, G., Sánchez-Mateos, P., Sánchez-Madrid, F. and Arroyo, A. G. (2005). Membrane type 1-matrix metalloproteinase is involved in migration of human monocytes and is regulated through their interaction with fibronectin or endothelium. *Blood* **105**, 3956-3964.

Meyer, A. S., Hughes-Alford, S. K., Kay, J. E., Castillo, A., Wells, A., Gertler, F. B. and Lauffenburger, D. A. (2012). 2D protrusion but not motility predicts growth factor-induced cancer cell migration in 3D collagen. *J. Cell Biol.* **197**, 721-729.

Murphy, D. A. and Courtneidge, S. A. (2011). The 'ins' and 'outs' of podosomes and invadopodia: characteristics, formation and function. *Nat. Rev. Mol. Cell Biol.* **12**, 413-426.

Nakada, M., Miyamori, H., Yamashita, J. and Sato, H. (2003). Testican 2 abrogates inhibition of membrane-type matrix metalloproteinases by other testican family proteins. *Cancer Res.* **63**, 3364-3369.

Nourshargh, S., Hordijk, P. L. and Sixt, M. (2010). Breaching multiple barriers: leukocyte motility through venular walls and the interstitium. *Nat. Rev. Mol. Cell Biol.* **11**, 366-378.

Olkkonen, V. M., Dupree, P., Killisch, I., Lütcke, A., Zerial, M. and Simons, K. (1993). Molecular cloning and subcellular localization of three GTP-binding proteins of the rab subfamily. *J. Cell Sci.* **106**, 1249-1261.

Pellinen, T., Arjonen, A., Vuoriluoto, K., Kallio, K., Fransen, J. A. and Ivaska, J. (2006). Small GTPase Rab21 regulates cell adhesion and controls endosomal traffic of beta1-integrins. *J. Cell Biol.* **173**, 767-780.

Petrie, R. J., Gavara, N., Chadwick, R. S. and Yamada, K. M. (2012). Nonpolarized signaling reveals two distinct modes of 3D cell migration. *J. Cell Biol.* **197**, 439-455.

Pixley, F. J. (2012). Macrophage migration and its regulation by CSF-1. *Int. J. Cell Biol.* **2012**, 501962.

Poincloux, R., Lizárraga, F. and Chavrier, P. (2009). Matrix invasion by tumour cells: a focus on MT1-MMP trafficking to invadopodia. *J. Cell Sci.* **122**, 3015-3024.

Remacle, A., Murphy, G. and Roghi, C. (2003). Membrane type I-matrix metalloproteinase (MT1-MMP) is internalised by two different pathways and is recycled to the cell surface. *J. Cell Sci.* **116**, 3905-3916.

Remacle, A. G., Rozanov, D. V., Fugere, M., Day, R. and Strongin, A. Y. (2006). Furin regulates the intracellular activation and the uptake rate of cell surface-associated MT1-MMP. *Oncogene* **25**, 5648-5655.

Remacle, A. G., Golubkov, V. S., Shiryaev, S. A., Dahl, R., Stebbins, J. L., Chernov, A. V., Cheltsov, A. V., Pellecchia, M. and Strongin, A. Y. (2012). Novel MT1-MMP small-molecule inhibitors based on insights into hemopexin domain function in tumor growth. *Cancer Res.* **72**, 2339-2349.

Sabeh, F., Shimizu-Hirota, R. and Weiss, S. J. (2009). Protease-dependent versus -independent cancer cell invasion programs: three-dimensional amoeboid movement revisited. *J. Cell Biol.* **185**, 11-19.

Sakurai-Yageta, M., Recchi, C., Le Dez, G., Sibarita, J. B., Daviet, L., Camonis, J., D'Souza-Schorey, C. and Chavrier, P. (2008). The interaction of IQGAP1 with the exocyst complex is required for tumor cell invasion downstream of Cdc42 and RhoA. *J. Cell Biol.* **181**, 985-998.

Sato, H., Kinoshita, T., Takino, T., Nakayama, K. and Seiki, M. (1996). Activation of a recombinant membrane type 1-matrix metalloproteinase (MT1-MMP) by furin and its interaction with tissue inhibitor of metalloproteinases (TIMP)-2. *FEBS Lett.* **393**, 101-104.

Schlierf, B., Fey, G. H., Hauber, J., Hocke, G. M. and Rosorius, O. (2000). Rab11b is essential for recycling of transferrin to the plasma membrane. *Exp. Cell Res.* **259**, 257-265.

Schwartz, S. L., Cao, C., Pylypenko, O., Rak, A. and Wandinger-Ness, A. (2007). Rab GTPases at a glance. *J. Cell Sci.* **120**, 3905-3910.

Simpson, J. C., Griffiths, G., Wessling-Resnick, M., Fransen, J. A., Bennett, H. and Jones, A. T. (2004). A role for the small GTPase Rab21 in the early endocytic pathway. *J. Cell Sci.* **117**, 6297-6311.

Sithu, S. D., English, W. R., Olson, P., Krubasik, D., Baker, A. H., Murphy, G. and D'Souza, S. E. (2007). Membrane-type 1-matrix metalloproteinase regulates intracellular adhesion molecule-1 (ICAM-1)-mediated monocyte transmigration. *J. Biol. Chem.* **282**, 25010-25019.

Sönnichsen, B., De Renzis, S., Nielsen, E., Rietdorf, J. and Zerial, M. (2000). Distinct membrane domains on endosomes in the recycling pathway visualized by multicolor imaging of Rab4, Rab5, and Rab11. *J. Cell Biol.* **149**, 901-914.

Stanton, H., Gavrilovic, J., Atkinson, S. J., d'Ortho, M. P., Yamada, K. M., Zardi, L. and Murphy, G. (1998). The activation of ProMMP-2 (gelatinase A) by HT1080 fibrosarcoma cells is promoted by culture on a fibronectin substrate and is concomitant with an increase in processing of MT1-MMP (MMP-14) to a 45 kDa form. *J. Cell Sci.* **111**, 2789-2798.

Steffen, A., Le Dez, G., Poincloux, R., Recchi, C., Nassoy, P., Rottner, K., Galli, T. and Chavrier, P. (2008). MT1-MMP-dependent invasion is regulated by TI-VAMP/VAMP7. *Curr. Biol.* **18**, 926-931.

Stein, M. P., Dong, J. and Wandinger-Ness, A. (2003). Rab proteins and endocytic trafficking: potential targets for therapeutic intervention. *Adv. Drug Deliv. Rev.* **55**, 1421-1437.

Stenmark, H. (2009). Rab GTPases as coordinators of vesicle traffic. *Nat. Rev. Mol. Cell Biol.* **10**, 513-525.

Stenmark, H., Parton, R. G., Steele-Mortimer, O., Lütcke, A., Gruenberg, J. and Zerial, M. (1994). Inhibition of rab5 GTPase activity stimulates membrane fusion in endocytosis. *EMBO J.* **13**, 1287-1296.

Tatin, F., Varon, C., Génot, E. and Moreau, V. (2006). A signalling cascade involving PKC, Src and Cdc42 regulates podosome assembly in cultured endothelial cells in response to phorbol ester. *J. Cell Sci.* **119**, 769-781.

van der Sluijs, P., Mohrmann, K., Deneka, M. and Jongeneelen, M. (2001). Expression and properties of Rab4 and its effector rabaptin-4 in endocytic recycling. *Methods Enzymol.* **329**, 111-119.

Van Goethem, E., Poincloux, R., Gauffre, F., Maridonneau-Parini, I. and Le Cabec, V. (2010). Matrix architecture dictates three-dimensional migration modes of human macrophages: differential involvement of proteases and podosome-like structures. *J. Immunol.* **184**, 1049-1061.

van Hinsbergh, V. W., Engelse, M. A. and Quax, P. H. (2006). Pericellular proteases in angiogenesis and vasculogenesis. *Arterioscler. Thromb. Vasc. Biol.* **26**, 716-728.

Vérollet, C., Charrière, G. M., Labrousse, A., Cougoule, C., Le Cabec, V. and Maridonneau-Parini, I. (2011). Extracellular proteolysis in macrophage migration: losing grip for a breakthrough. *Eur. J. Immunol.* **41**, 2805-2813.

Wiesner, C., Faix, J., Himmel, M., Bentzien, F. and Linder, S. (2010). KIF5B and KIF3A/KIF3B kinesins drive MT1-MMP surface exposure, CD44 shedding, and extracellular matrix degradation in primary macrophages. *Blood* **116**, 1559-1569.

Williams, K. C. and Coppolino, M. G. (2011). Phosphorylation of membrane type 1-matrix metalloproteinase (MT1-MMP) and its vesicle-associated membrane protein 7 (VAMP7)-dependent trafficking facilitate cell invasion and migration. *J. Biol. Chem.* **286**, 43405-43416.

Wolf, K. and Friedl, P. (2005). Functional imaging of pericellular proteolysis in cancer cell invasion. *Biochimie.* **87**, 315-320.

Wolf, K. and Friedl, P. (2009). Mapping proteolytic cancer cell-extracellular matrix interfaces. *Clin. Exp. Metastasis* **26**, 289-298.

Wolf, K. and Friedl, P. (2011). Extracellular matrix determinants of proteolytic and non-proteolytic cell migration. *Trends Cell Biol.* **21**, 736-744.

Wolf, K., Mazo, I., Leung, H., Engelke, K., von Andrian, U. H., Deryugina, E. I., Strongin, A. Y., Bröcker, E. B. and Friedl, P. (2003). Compensation mechanism in tumor cell migration: mesenchymal-amoeboid transition after blocking of pericellular proteolysis. *J. Cell Biol.* **160**, 267-277.

Wolf, K., Wu, Y. I., Liu, Y., Geiger, J., Tam, E., Overall, C., Stack, M. S. and Friedl, P. (2007). Multi-step pericellular proteolysis controls the transition from individual to collective cancer cell invasion. *Nat. Cell Biol.* **9**, 893-904.

Yamamoto, H., Koga, H., Katoh, Y., Takahashi, S., Nakayama, K. and Shin, H. W. (2010). Functional cross-talk between Rab14 and Rab4 through a dual effector, RUFY1/Rabip4. *Mol. Biol. Cell* **21**, 2746-2755.

Yudowski, G. A., Puthenveedu, M. A., Henry, A. G. and von Zastrow, M. (2009). Cargo-mediated regulation of a rapid Rab4-dependent recycling pathway. *Mol. Biol. Cell* **20**, 2774-2784.

Zerial, M. and McBride, H. (2001). Rab proteins as membrane organizers. *Nat. Rev. Mol. Cell Biol.* **2**, 107-117.